applied sciences

MDPI

Article

Thermal Behavior of Biodegradable Compositions of Polylactide and Poly(3-hydroxybutyrate) with Chitosan and the Effect of UV Radiation on Their Structure

Svetlana Rogovina [1,*], Sergei Lomakin [1,2,*], Sergey Usachev [1], Anastasia Yakhina [1], Lubov Zhorina [1] and Alexander Berlin [1]

[1] N. N. Semenov Federal Research Center for Chemical Physics, Academy of Science, 119991 Moscow, Russia
[2] N. M. Emanuel Institute of Biochemical Physics, Russian Academy of Sciences, 119334 Moscow, Russia
* Correspondence: s.rogovina@mail.ru (S.R.); lomakin@sky.chph.ras.ru (S.L.)

Abstract: The negative influence of water pollution by heavy metals ions on human health represents a serious ecological problem which requires effective methods in the search for its solution. The creation of eco-friendly biodegradable polymer materials capable of performing the sorption of the water media of heavy metals followed by decomposition into harmless substances after the end of their service life presents an actual task. To this aim, binary compositions synthesized from natural raw polyesters polylactide (PLA) and poly(3-hydroxybutyrate) (PHB) with polysaccharide chitosan, corresponding to these requirements, were obtained in the liquid phase. The polyesters have mechanical characteristics close to the characteristics of synthetic polymers, while the chitosan containing the amino groups is capable of performing the sorption of heavy metals. The use of compositions on their base allows one to create the new inexpensive biodegradable sorbents stable in aqueous media as well as apply them as packing materials. The sorption capacity of PLA–chitosan and PHB–chitosan compositions in relation to iron ions from aqueous solutions was explored by a method of X-ray fluorescence analysis and it was established that the sorption of Fe^{3+} ions by PHB–chitosan composition is more than twice as high as that by the PLA–chitosan composition (2.30 and 0.66 wt. %, correspondingly, after sorption from 0.008 mol/L $FeCl_3$ solution during 24 h). A comparative study of thermophysical parameters and the degree of crystallinity of PLA and PHB, as well as in their initial compositions and compositions, containing sorbed iron ions, was carried out by DSC method. The DSC analysis of the PLA–chitosan and PHB–chitosan compositions, containing sorbed iron ions, showed a slight decrease in the values of Tg, T_{cc}, and T_m as well as an increase in the enthalpy of cold crystallization and a reduction in the degree of crystallinity of these polyesters. At the same time, an increasing of the thermal stability of polyester compositions in the presence of iron ions was established. The influence of UV irradiation on the structure of PLA and PHB for 2, 5, 24, and 144 h was analyzed by FTIR spectroscopy and significant changes in the spectrum were observed. Based on the analysis of the IR spectra of PHB and PLA, it was concluded that, under the action of UV radiation, the destruction of ester bonds takes place, which is expressed in the appearance of intense bands characterizing the formation of new structural units, resulting in the decrease in the molecular weight of polyesters.

Keywords: polylactide; poly(3-hydroxybutyrate); chitosan; composite films; sorption of iron ions; thermal transitions; UV radiation

check for updates

Citation: Rogovina, S.; Lomakin, S.; Usachev, S.; Yakhina, A.; Zhorina, L.; Berlin, A. Thermal Behavior of Biodegradable Compositions of Polylactide and Poly(3-hydroxybutyrate) with Chitosan and the Effect of UV Radiation on Their Structure. *Appl. Sci.* **2023**, *13*, 3920. https://doi.org/10.3390/app13063920

Academic Editor: Ludmila L. Semenycheva

Received: 15 February 2023
Revised: 12 March 2023
Accepted: 13 March 2023
Published: 20 March 2023

Copyright: © 2023 by the authors. Licensee MDPI, Basel, Switzerland. This article is an open access article distributed under the terms and conditions of the Creative Commons Attribution (CC BY) license (https://creativecommons.org/licenses/by/4.0/).

1. Introduction

The development of biodegradable polymer composition materials which can decompose under the action of the environment significantly reduces the negative influence of petrol-based polymers on ecosystems [1–3]. Among the various numerous fields of their application, the biobased polymer systems can be successfully used for the creation of absorbents for the purification of an aquatic environment from industrial waste including

toxic heavy metals, particularly iron, which negatively influences human health. According to the requirements of the European Union, the maximum total content of Fe^{3+} should not exceed 1.0–1.5 mg/L [4].

At the same time, such methods of water purification of metals including precipitation or flocculation are the low efficiency and demand for the substitution of new, ecologically safe, and efficient sorbents with high productivity. In this connection, the development of sorbents based on the eco-friendly polymers of different classes is a new approach to the solution of this problem.

Biodegradable polysaccharide chitosan, obtained by the deacetylation of natural polysaccharide chitin and due to presence of amino groups, possesses a good sorption ability that explains its successful application as a sorbent of heavy metals, including iron [5,6], but its significant swelling in aqueous media leads to a decrease in the mechanical characteristics [7,8].

On the other hand, the polyesters polylactide (PLA) and poly(3-hydroxybutyrate) (PHB) derived from natural raw materials as well as their compositions are widely used in various fields [9–14]. According to European Bioplastics [15], the total global production capacity of bioplastics in 2021 was 2.42 million tons. Out of this, the production of PLA was 18.9%. However, the applications of PLA and PHB are limited by their fragility, which is due to their high crystallinity, low thermal stability, and the low differences between their melting and thermal decomposition temperatures [16–18]. In this connection, the use of chitosan in compositions with PLA and PHB allows one to obtain biodegradable materials that combine good mechanical characteristics along with a high sorption capacity that determines the prospects of their use as the sorbents of heavy metals from wastewater. The main advantage of such compositions as compared with compositions based on synthetic polymers is their ability to remain biodegradable after the end of their exploitation period, which determines their use as environmentally safe materials.

Additionally, as is well known, food packing films used for containing, protecting and prolonging the life of food, which are prepared from petroleum-based raw polymers, cause serious pollution in oceans, lakes, rivers, and agricultural lands [19]. Moreover, this requires determining how the synthetic polymers prepared from petroleum-based raw polymers can be completely replaced by natural polymers, which is also currently a very demanding task. [20,21].

Earlier, we carried out a comparative study of the thermal properties of binary polyester compositions PLA–PHB [22], as well as the sorption capacity of the ternary compositions PLA–PHB–chitosan with respect to Fe^{3+} ions [23], prepared from petroleum-based raw polymers, which cause serious pollution in oceans, lakes, rivers, and agricultural lands. The choice of such compositions was connected with the fact that the polyesters PLA and PHB, which perform reinforcing functions, provide stability to the compositions with chitosan in aqueous media. At the same time, PLA is a cheaper polymer than PHB, while PHB demonstrates an increased ability to biodegrade its base articles after the end of its service life. Since ternary compositions do not allow for the precise determination of the role of their polyesters in the processes occurring during the sorption of metals from aqueous media, a study of the hydrolysis, biodegradation, and sorption capacity of dual-film compositions, namely PLA–chitosan and PHB–chitosan with respect to iron ions was carried out in [24]. It was shown that the PLA–chitosan compositions have greater stability in acidic aqueous media, increased sorption capacity with respect to iron ions, and, at the same time, are more easily degraded under exposure to soil after end of their service life, i.e., they show better characteristics for their use as the sorbents of iron ions. This may be connected to the difference in polarity and crystallinity of polyesters, and thus, with the various interactions between the ester groups of polyesters and amino groups of chitosan.

It should be noted that materials based on polyesters and chitosan could be used not only as metal sorbents, but also for food packaging. The basic role of food packing nowadays is to preserve and protect food products from the aggressive action of the environment, including UV radiation, which falls within 100–400 nm of the electromagnetic

spectrum. Generally, the UV-range is divided into sub-regions, namely UV-A (315–400 nm), UV-B (280–315 nm), and UV-C (100–280) nm. The most rigid UV-C range is intensely absorbed by ozone, oxygen, and carbon dioxide as sunlight passes through the Earth's atmosphere. As a result, people and the environment are exposed to higher levels of UV-B radiation, and it is UV-B rays that have the most adverse effects on human health, animals, marine organisms, and plant life.

UV radiation may also destroy films for food packing, resulting, for example, in lipid oxidation, color and odor changes in products, and vitamin degradation [25]. On the other hand, UV has been used in the food industry as a sterilizer and antifungal agent germicide [26].

The purpose of the present work was a comparative study of the thermal stability and the thermophysical transitions in the binary polyester–chitosan compositions as well as in their compositions containing sorbed iron ions. In studying of the influence of UV radiation on the structural changes of PHB and PLA, special attention was paid to the analysis and interpretation of their infrared spectra.

The obtained results make it possible to predict the behavior of such compositions under negative environmental conditions when they are used as sorbents or packing materials.

2. Materials and Methods

2.1. Materials

PLA 4043D pellets with diameter of 3 mm (M_w = 2.2 × 10^5, M_n = 1.65 × 10^5, T_m = 155 °C, polydispersity index D = M_w/M_n = 1.35, transparency 2.1%) were obtained from Nature Works (Minnetonka, MN, USA); PHB («Biomer», Kreilling, Germany) (M_w = 2.05 × 10^5, T_m = 175 °C), chitosan produced by Bioprogress (Shchelkovo, Moscow, Russia, M_w = 4.4 × 10^5, degree of deacetylation 0.87), and anhydrous ferric chloride (Fluka Chemie, Buchs, Switzerland) were used.

2.2. Production of Compositions

Films were prepared by mixing PLA and PHB solutions in chloroform, in which chitosan powder under mechanical stirring was introduced. The resulting films with a component ratio (50:50) wt. % and a thickness of 0.2–0.3 mm were dried at room temperature. For the investigation of the sorption of iron ions by composition films, they were placed in aqueous solutions of $FeCl_3$ in various concentrations and kept in solutions for a certain time, after which they were dried at a temperature of 50–60 °C.

2.3. X-ray Fluorescence Analysis

The percentage of Fe in the compositions subjected to sorption was determined by X-ray fluorescence analysis on an X-ray fluorescence wave-dispersive spectrometer ARL PERFORM'X, model ARL PFX-101 (Switzerland).

The spectrometer consists of an X-ray source, a device for installing test samples, a dispersing system, a secondary radiation receiver, and electronic units. The spectrometer uses an X-ray tube with an Rh anode, a voltage of 50 kV, and a current of 30 mA as an X-ray source.

The excitation of the sample's secondary (characteristic) radiation falls in the LiF-analyzer crystal. As a result of diffraction on the crystal, the radiation is decomposed into a spectrum (according to Bragg's law). The spectrometer performs the point analysis of samples with a beam of 3 mm in diameter with a step of 0.1 mm, and builds a map of the distribution of elements over the surface of the sample. The mass concentration of elements is determined from the position and intensity of the lines in the spectrum. The parameters are calculated according to the reference-free methodology for the quantitative calculation of element concentrations.

The sample weights were approximately 200 mg. The preparation of samples included three successive cycles: grinding samples in a porcelain mortar with a pestle; the addition

of polyvinyl alcohol; and pressing a tablet with a diameter of 3 mm. The spectra were recorded and all further manipulations were performed using the SIALMO.UQ method.

2.4. Thermophysical Properties

The thermophysical characteristics and the thermal stability of polymers in the initial mixtures and compositions containing sorbed iron ions were studied by the differential scanning calorimetry (DSC) method on a DSC-204 F1 (Netzsch, Holding KG, Selb, Germany) calorimeter at the heating rate 10 K/min in an inert atmosphere of gas argon in the temperature range of 25–200 °C. The experiments included several consecutive cycles: the first heating, cooling, and second heating at the same rate. The specific heat flux from the melting peak (mW/mg) was corrected for the weight of PLA and PHB in the composition with chitosan. The degree of crystallinity, χ%, taking into account the mass fraction of PLA in the compositions (α = 0.5), was calculated by the equation:

$$\chi = \frac{\Delta H_m - \Delta H_{cc}}{\Delta H_m^{100} \times \alpha}, \quad (1)$$

where ΔH_m-enthalpy of melting; ΔH_{cc}-enthalpy of crystallization (enthalpy of "cold" crystallization); and ΔH_m^{100}—the theoretical value of the 100%-crystalline poly(L-lactide) melting enthalpy (93.6 J/g) [27].

The calculations of the degree of crystallinity of PHB and its composition with chitosan did not take into account the enthalpy of "cold" crystallization. The melting enthalpy of 100% crystalline PHB, according to the literature data, was taken as 146 J/g [28].

The use of a repeating heating–cooling mode in DSC studies of polymers in order to remove the "prehistory" of their production is generally accepted. In this work, DSC studies were carried out without a reheating procedure, since the desorption of water weakly bounded to the amino groups of chitosan followed by a weight loss of 12 wt. % occurs at a temperature lower than the melting temperature of polyesters [29,30]. Therefore, the procedures of cooling and reheating in the DSC losing mode is meaningless due to quantitative and qualitative composition changes.

2.5. UV Radiation

The exposure of the composite films to ultraviolet (UV) radiation was performed at a wavelength of 253.7 nm and with a lamp power of 11 W (4 Philips TUV lamps) for 2, 5, 24, and 144 h.

2.6. Investigation of Polymers by FTIR-Spectroscopy

The infrared spectra of the polyesters PLA and PHB both before and after the UV-radiation has acted on them were acquired with the aid of Bruker Tensor 27 IR Fourier spectrometer with ATR PIKE Miracles™ accessory (PIKE Technologies, Madison, WI, USA) equipped with a germanium (Ge) crystal. IR spectra were recorded in the range of 4000–700 cm^{-1} with a resolution of 4 cm^{-1} and averaging over 32 successive scans.

The obtained infrared spectra were interpreted using characteristic frequency values for PLA and PHB, which were described in the literature [31–39].

3. Results and Discussion

3.1. The Comparison of Sorption Capacity of PHB–Chitosan and PLA–Chitosan Compositions

The use of the biodegradable binary polymer compositions PHB–chitosan and PLA–chitosan as sorbents of metals from wastewater is one of their promising application directions, representing a large potential interest due to possibility of utilizing these polymers after the end of their service life.

Table 1 shows the quantitative characteristics of iron ions' sorption by PHB–chitosan and PLA–chitosan film compositions from $FeCl_3$ solutions with different concentrations of time, obtained by the method of X-ray fluorescence analysis, which is described above

in the division Materials and Methods. The mass concentration of absorbed iron ions was determined by the position and intensity of the lines in the diffraction spectrum.

Table 1. The concentration of sorbed Fe^{3+} ions (wt. %) by the film compositions PHB–chitosan (50:50) wt. % and PLA–chitosan (50:50) wt. %.

Concentration of $FeCl_3$, Solutions, mol/L	Time of Sorption, h					
	0.5	**2**	**4**	**8**	**16**	**24**
PHB–Chitosan						
0.002	0.10	0.19	0.36	0.41	0.40	0.42
0.005	0.22	0.48	0.97	0.97	1.31	1.24
0.008	0.39	0.75	1.32	2.08	2.20	2.30
PLA–Chitosan						
0.002	0.03	0.07	0.09	0.13	0.15	0.11
0.005	0.03	0.06	0.08	0.56	0.48	0.51
0.008	0.05	0.12	0.37	0.85	0.89	0.66

As can be seen from Table 1, a growth in the $FeCl_3$ concentration in the solutions leads to an increase in the amount of sorbed iron ions. At the same time the sorption capacity of binary PHB–chitosan compositions is more than twice as high than in PLA–chitosan compositions. This can be explained by the fact that, although PLA and PHB have the same functional groups and repeating units in their chains, their properties slightly differ from each other and, in addition, the crystallinity of PHB is higher than that of PLA. For these reasons, the molecules of polyesters in various degrees screen the- NH_2- groups of chitosan, that are affected by its sorption capacity.

In this connection, a comparative study of the thermophysical behavior of these compositions and the determination of thermophysical characteristics both in the absence and in the presence of sorbed iron ions and the evaluation of their influence on the relevant process parameters was carried out.

3.2. Thermophysical Characteristics of PHB–Chitosan and PLA–Chitosan Compositions

The thermal behavior and thermal stability of PLA, PHB, and their compositions with chitosan, as well as the compositions PLA–chitosan and PHB–chitosan with absorbed Fe^{3+} ions was investigated by the DSC method in the temperature range of 30–400 °C.

Figures 1 and 2 show the typical DSC thermograms obtained for plain PLA, PHB, chitosan, PLA–chitosan (50:50) wt. %, PHB–chitosan (50:50) wt. %, as well as for the same compositions containing absorbed Fe^{3+} ions in the amounts of 0.89 and 2.20 wt. %, correspondingly. Table 2 summarizes the main DSC parameters: glass transition T_g, peak temperatures for cold crystallization T_{cc} and melting T_m, characteristic enthalpies associated with cold crystallization ΔH_{cc} and melting ΔH_m, as well as the degree of crystallization (χ, %, Equation (1)) (Supplementary Materials, Calculation of the thermophysical parameters obtained by DSC).

From the PLA data presented in Figure 1 and Table 2, a glass transition can be observed at 65 °C, as well as two melting peaks with temperatures of 146.0 °C and 163.3 °C, related to α' (imperfect) and α (perfect) crystalline forms of PLA, respectively. The absence of a cold crystallization peak on the DSC curve should be noted, which indicates a relatively high degree of crystallinity of the initial PLA (χ = 43.2%) (Table 2). In contrast to plain PLA, the glass transition temperature of PLA in composition with chitosan decreases by 2 °C, and the melting peaks related to α' (imperfect) and α (perfect) PLA crystalline forms are 154.0 °C and 161.5 °C, respectively, and the crystallinity degree (χ, %) is lower by 43% (from 43.2 to 24.6). In this regard, one can conclude that, in the process of producing a PLA–chitosan composition in the solution, the original polylactide is amorphized.

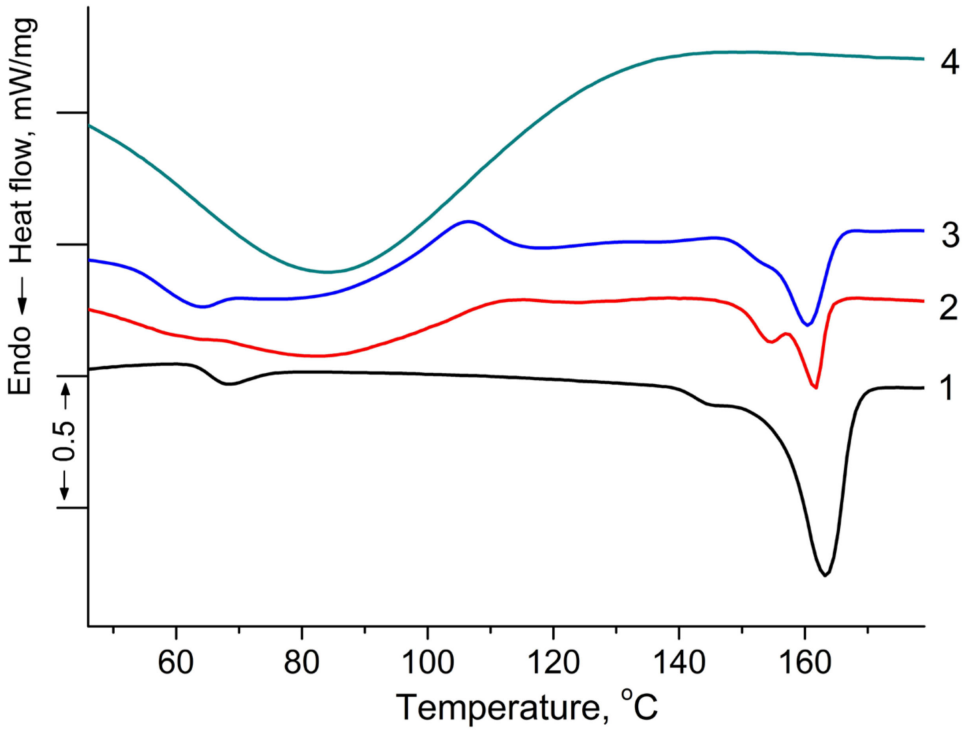


Figure 1. DSC heat flow curves of PLA: (1) PLA–chitosan (50:50) wt. % and (2) PLA–chitosan (50:50); wt. % compositions containing sorbed Fe^{3+} ions (3) and original chitosan (4).

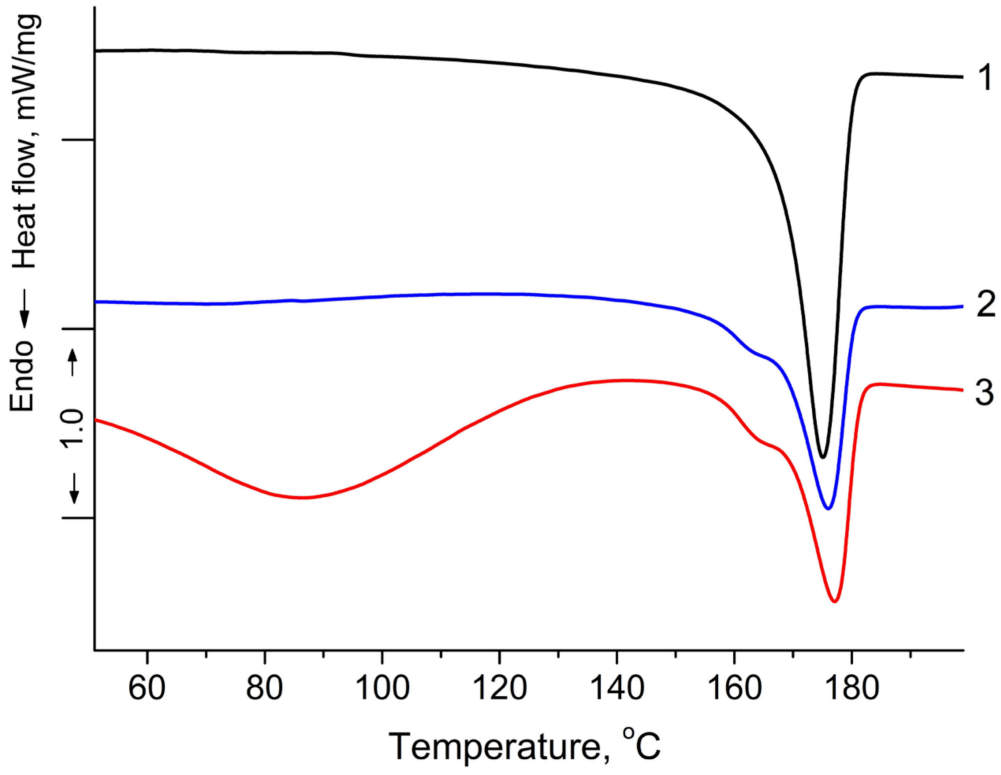


Figure 2. DSC heat flow curves of PHB (1), PHB–chitosan (50:50) wt. % (2) and PHB–chitosan (50:50) wt. % composition containing sorbed Fe^{3+} ions (3).

Table 2. DSC parameters of thermal transitions observed in PLA, PHB, and their compositions with chitosan (Supplementary Materials: Calculation of thermophysical parameters obtained by DSC).

Sample	T_g, °C	T_{cc}, °C	ΔH_{cc}, J/g	T_m, °C	ΔH_m, J/g	χ, %
PLA	65.0	-	-	146.0/163.3	40.5	43.2
PHB	-	-	-	175.0	−92.7	63.5
PLA–chitosan	62.8	113.7	6.1	155.0/161.5	−29.2	24.6
PHB–chitosan	-	-	-	165.4/177.7	−75.2	51.5
PLA–chitosan Fe^{3+} sorbed	61.3	107.0	12.6	154.0/160.8	−34.1	22.9
PHB–chitosan Fe^{3+} sorbed	-	-	-	165.0/176.0	−73.0	50.0

This DSC analysis of the PLA–chitosan composition containing sorbed Fe^{3+} shows a slight decrease in the values of T_g, T_{cc}, and T_m, as well as an increase in the enthalpy of "cold crystallization" ΔH_{cc} = 12.6 J/g as compared to the initial composition PLA–chitosan. As a result, the degree of PLA crystallinity absorbed in the composition PLA–chitosan with Fe^{3+} slightly decreases (Table 2).

The DSC analysis of the PHB–chitosan compositions (Figure 2) shows that, in contrast to the initial PHB, the presence of chitosan and sorbed Fe^{3+} ions in the compositions leads to the appearance of an additional small endo-peak with a temperature of 165 °C, which can be attributed to the melting of the imperfect form of PHB crystallites.

At the same time, the degree of PHB crystallinity in the PHB–chitosan composition decreases to 18.9%, and in the PHB–chitosan compositions with sorbed Fe^{3+} ions, it decreases to 21.3% compared to the initial PHB (Table 2). This indicates the amorphization of PHB in compositions with chitosan during their liquid-phase preparation by analogy with PLA.

The thermal stability of PLA, PHB, and their compositions with chitosan has been studied using DSC. The onset temperature (T_{on}) of the thermal decomposition was determined according to the ISO 11357-1:2010-03 standard. The value of T_{on} has been defined as the calculated point of the intersection of the extrapolated baseline and the inflection tangent at the beginning of the degradation peak on the DSC curve. The data are shown in Figures 3 and 4 and in Table 3.

From the DSC data presented in Figure 3, the influence of chitosan on the sharp decrease in the onset thermal degradation temperature (T_{on}) of the PLA–chitosan composition and PLA–chitosan composition containing sorbed Fe^{3+} ions in contrast to original PLA: 237 °C, 244 °C and 332 °C, respectively, can be clearly seen. There is also a significant decrease (of approximately 100 °C) in the enthalpy peak (T_{max}) of the thermal decomposition of the PLA–chitosan and PLA–chitosan compositions containing absorbed Fe^{3+} ions compared with the original PLA: 269 °C, 275 °C, and 372 °C, respectively (Table 2).

At the same time, it is necessary to note the stabilizing effect of Fe^{3+} ions on PLA–chitosan thermal decomposition, which is clearly manifested under the comparison of the values of the decomposition enthalpy (ΔH_d) of PLA–chitosan and PLA–chitosan compositions containing absorbed Fe^{3+} ions (Table 3).

Figure 4 demonstrates the effect of the presence of chitosan on the thermal stability of PHB. However, unlike PLA compositions, the effect of chitosan on the decrease in T_{on} and T_{max} values for PHB–chitosan compositions is not so pronounced Thus, the value of T_{on} for PHB gradually decreases from 264 °C (PHB) to 255 °C (PHB–chitosan (50:50) wt. %) and 246 °C for the PHB–chitosan composition with sorbed Fe^{3+} ions (Table 3). On the other hand, from the data presented in Table 2, the stabilizing factor of Fe^{3+} ions in the process of PHB with chitosan thermal decompositions can be clearly observed. This is expressed in an increase in the values of T_{max} and ΔH_d for the composition of PHB–chitosan with adsorbed Fe^{3+} ions (278 °C and −687 J/g) in comparison with the analogous values of 268 °C and −584 J/g for the PHB–chitosan composition (Table 3).

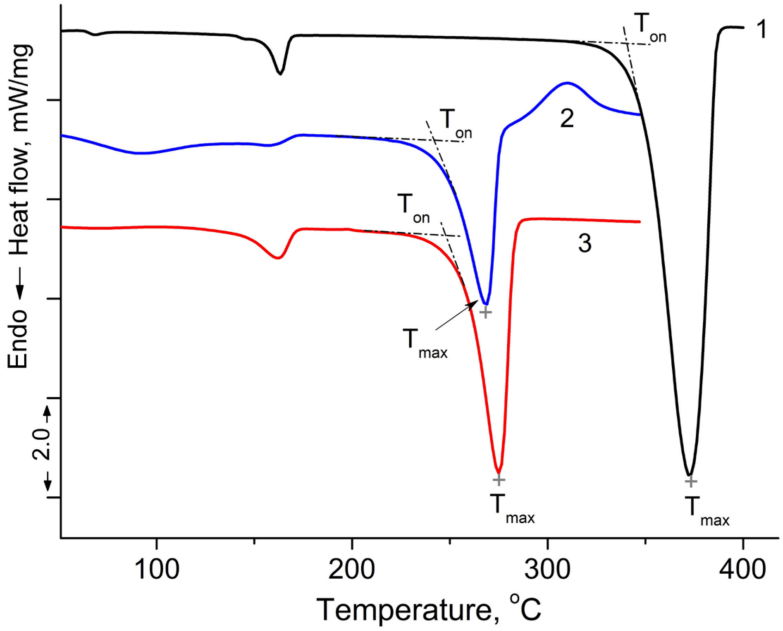


Figure 3. DSC heat flow curves of PLA (1), PLA–chitosan (50:50) wt. % composition (2) and PLA–chitosan (50:50) wt. % composition containing sorbed Fe^{3+} ions (3), obtained by heating up to 400 °C.

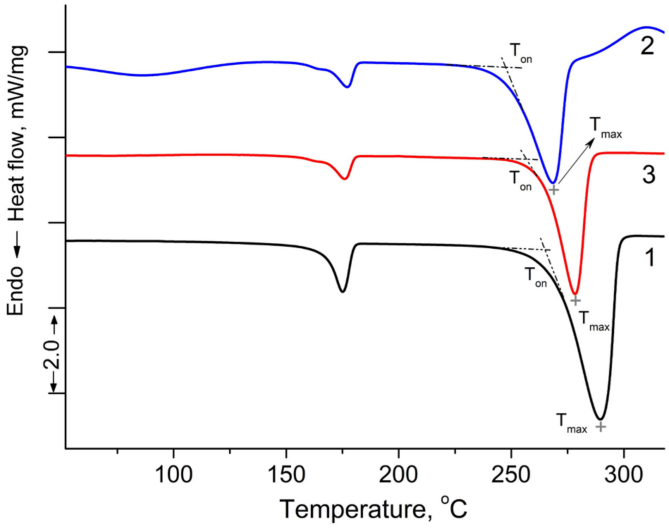


Figure 4. DSC heat flow curves of PHB (1), PHB–chitosan (50:50) wt. % composition (2) and PHB–chitosan (50:50) wt. % composition containing sorbed Fe^{3+} ions (3), obtained by heating up to 400 °C.

Table 3. Thermal stability characteristics of PLA and PHB and their compositions with chitosan (Supplementary Materials: Calculation of the thermophysical parameters obtained by DSC).

Sample	T_{on}, °C	T_{max}, °C	ΔH_d, J/g
PLA	332	372	−1229
PLA–chitosan (50:50)	237	269	−700
PLA–chitosan (50:50) Fe^{3+} absorbed	244	275	−1214
PHB	264	290	−730
PHB–chitosan (50:50)	255	268	−584
PHB–chitosan (50:50) Fe^{3+} absorbed	246	278	−687

At the same time, the analysis of the DSC (Figures 3 and 4, Table 2) leads to the conclusion about the common nature of the destabilizing effect of chitosan on the process of PLA and PHB thermal degradation.

Apparently, the reason for such a significant decrease in the thermal stability of PLA and PHB in their compositions with chitosan is connected to the presence of free chitosan amino groups, which accelerate the hydrolysis and depolymerization of linear polyesters.

3.3. Investigation of the Uvradiation Action on Polyesters PHB and PLA by a Method of IR Spectroscopy

The chemical structure of PLA and PHB exposed to UV-C radiation for 2, 5, 24, and 144 h was studied with the use of FTIR spectroscopy. It was found that the spectral characteristics of chitosan, subjected to UV radiation, remained practically unchanged, in contrast to PLA and PHB ones. For this reason, the analysis of the effect of UV radiation was carried out by the spectra of PLA and PHB only.

Figure 5 shows the changes in the IR spectra of PHB exposed to UV radiation. As can be seen in the figure, significant changes in spectrum structure occurred. The transformations already begin to appear after 2 h of radiation and are expressed in altering the shapes of the bands related to the stretching vibrations of the ester group C–O–C (1280 cm^{-1}, as shown in the Supplementary File as Figure S1 and Table S2) and asymmetric vibrations C–O–C (1332 cm^{-1}, Figure S1).

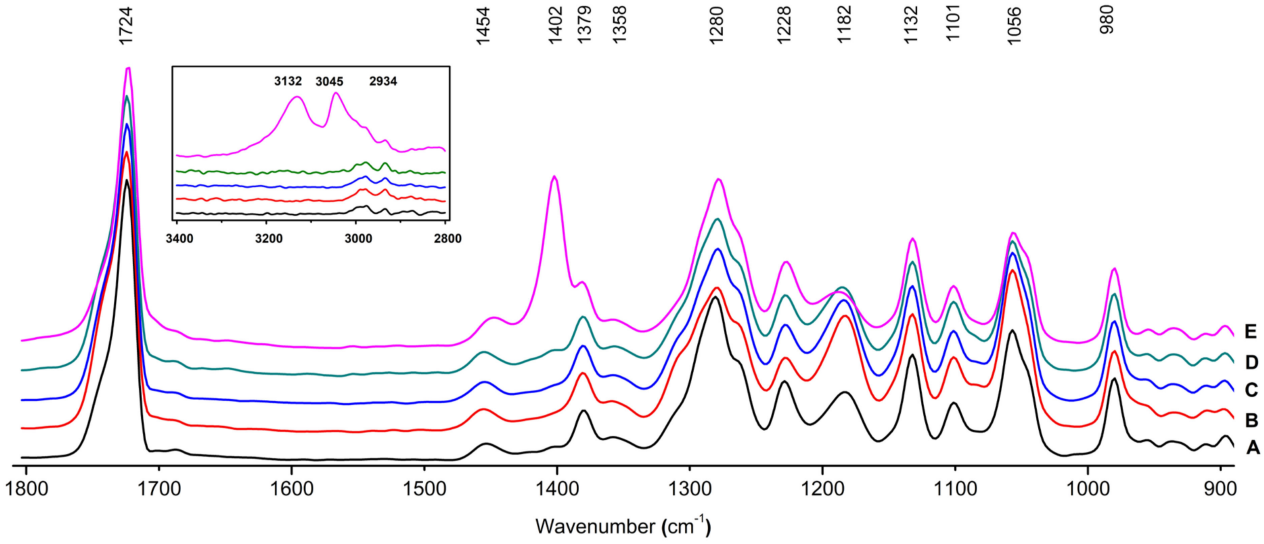


Figure 5. FTIR spectrum of PHB films before (A) and after UV radiation during 2 (B), 5 (C), 24 (D), 144 (E) hours.

There is also a change in the shape of the 1724 cm^{-1} (Figure S3 and Table S2) band relevant to the carbonyl group (C=O). At 1745 cm^{-1} (Figure S3), an additional spectral band is formed, indicating the presence of the C=O group, which is different from the original PHB. The band related to the stretching vibrations of the crystalline regions of the C–C bond (980 cm^{-1}, Figure S4 and Table S5) remains practically unchanged. There is no shift of the bands at 1379 cm^{-1} and 1358 cm^{-1} (Figure S1), which belong to the wagging vibrations and strain vibrations of the CH_3 group, respectively. The band at 1447 cm^{-1} (Figure S1), which is related to the asymmetric bending vibrations of the CH_3 group, is shifted by 6 cm^{-1} from the initial value of 1453 (1454) cm^{-1} (Figure S1), which is characteristic of the initial PHB. The greatest changes are observed in the samples after 144 h of UV radiation, expressed in the appearance of a band at 1402 cm^{-1} (Figure S1) and two broad bands at 3132 cm^{-1} and 3045 cm^{-1} (Figure 5). These three bands refer to the –OH stretching vibrations of the carboxyl group (Figure S4 and Table S5) and show that, after 144 h of UV irradiation of PHB

samples, a relative broadening and a decrease in the intensity of the band at 1182 cm^{-1} related to C–O–C vibrations in the amorphous region of the polymer takes place.

It can be assumed that the process of PHB photodegradation mainly affects the amorphous phase of the polymer, while the spectral region (1000–800 cm^{-1}) (Figure S6 and Table S7), characterizing the crystalline phase, remains practically unchanged.

Figure 6 shows the IR spectra of PLA exposed to UV radiation. As can be seen from figure, the most significant changes in the PLA spectrum are observed in the region of 1225–1170 cm^{-1}. This range is mixed and is defined by two bands with maxima at 1211 and 1184 cm^{-1} (Figure S8), related to asymmetric vibrations of the C–CO–O group and bending vibrations of CH_3 (Table S9). As the duration of UV radiation increases, their broadening occurs, which indicates a change in the structural features of this fragment. Bands at 1087 cm^{-1} and 1047 cm^{-1} are referred to as the symmetric vibrations of C–O–C groups and vibrations and of C–CH_3 stretching vibrations, respectively (Figure S8 and Table S9). The 1269 cm^{-1} band is mixed and consists of CH strain vibrations and C–CO–C stretching asymmetric vibrations (Table S9).

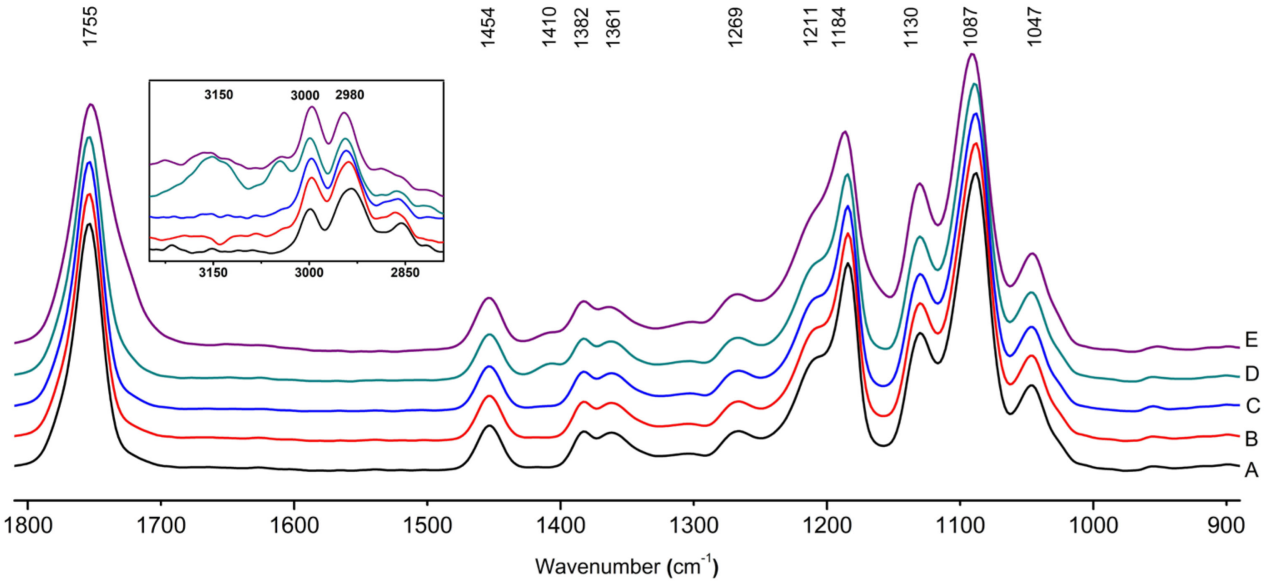


Figure 6. FTIR spectrum of PLA films before (A) and after UV radiation during 2 (B), 5 (C), 24, (D), 144 (E) hours.

The band at 1130 cm^{-1} refers to the asymmetric rocking vibrations of the CH_3-group (Figure S8 and Table S9). The regime of asymmetric strain vibrations of CH_3 appears at approximately 1454 cm^{-1} in the form of an intense band (Figure S10 and Table S11). The frequency stability reflects a pure asymmetric oscillation mode. The band at 1382 cm^{-1} refers to the symmetric strain vibrations of the CH_3-group [36]. The 1361 cm^{-1} band is mixed and consists of deformation and the asymmetric band vibrations of the CH in CH_3 group. After 24 h of UV radiation, new bands at 1410 cm^{-1} (Figure S10 and Table S11) and 3150 cm^{-1} (Figure 6) are observed in the PLA spectrum. These bands, as in the case of PHB (Figure 5), can be attributed to –OH vibrations in the carboxyl group. During the same period, changes also occur in the 1753 cm^{-1} band (Figure S12) related to the stretching vibrations of the carbonyl (C=O) group. Its broadening and the formation of a shoulder in the range of 1724 cm^{-1} are observed, which indicate the formation of a free carboxyl group due to the destruction of the ester group under the influence of UV irradiation.

Thus, based on a comparative analysis of the IR spectra of PHB and PLA, it can be concluded that, under the action of UV radiation, the destruction of the ester groups takes place, which is expressed in the appearance of intense bands characterizing the formation of new structural units. On the basis of obtaining the data, the formal mechanism of PHB

and PLA destruction under the action of ultraviolet radiation can be presented by the following scheme (Figure 7).

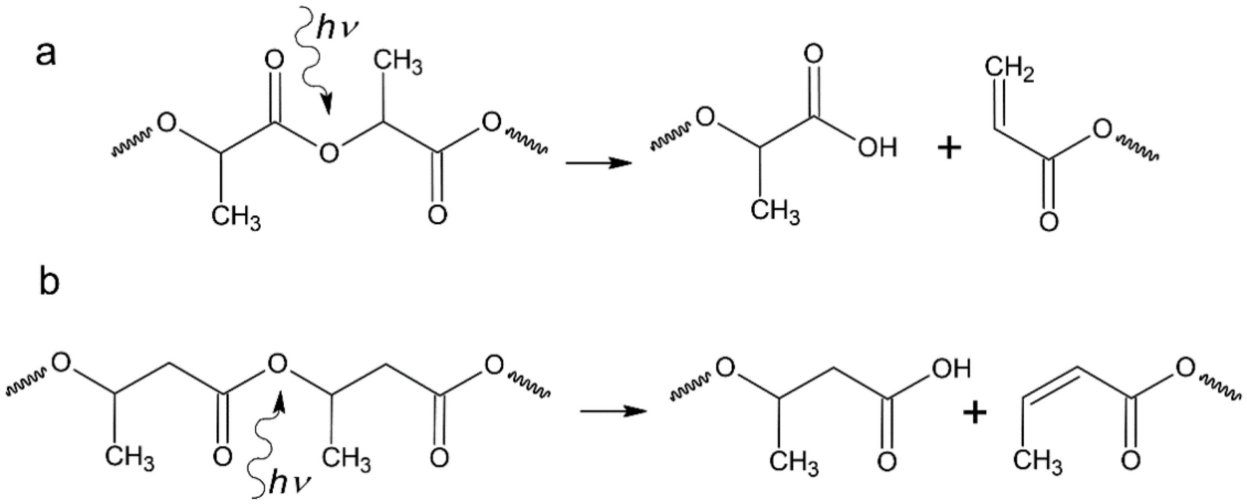


Figure 7. Scheme of PLA (**a**) and PHB (**b**) destruction under the action of UV radiation.

As such, the destruction of polyesters under the action of UV radiation occurs with the cleavage of the ester bonds. In this case, a free carboxyl group and an unsaturated bond in the α-position to the ester groups are formed, leading to a decrease in the molecular weight of polymers, the consequence of which is the embrittlement of the polymer composition observed after 144 h of UV radiation.

3.4. Statistical Analysis of FTIR Data

The statistical analysis of FTIR data (one-way ANOVA) related to the most significant results was obtained in this work using the trial version of OriginPro 2021 by OriginLab Co. The one-way statistical analysis of variance (ANOVA) was performed on the normalized spectral band intensities at 3145 and 3045 cm^{-1} for the PLA samples (Table 4, Figures 8 and 9), and at 3132 and at 3045 cm^{-1} for PHB samples (Table 5, Figures 10 and 11). These bands correspond to the largest changes in the spectra (–OH stretching vibrations of the carboxyl group), which suggests that the predominant scission of ester bonds occurs during the photodegradation process. Two pairs of practically unchanged UV irradiation bands (1379 cm^{-1} and 1358 cm^{-1} for PLA, as well as at 1379 cm^{-1} and 980 cm^{-1} for PHB) were chosen for comparison.

The results of the ANOVA test show the difference between the means and their variations for two clusters with a coefficient of variation of 0.52473, while the F factor of more than 10 for a level of significance 0.05 indicates that the variance of the reflection power densities in two different spectral line clusters have a cardinal statistically significant difference and the hypothesis of their correlated deviation nature is insignificant. A significant difference between the means and their variations for two clusters in the PHB sample with a F factor of 10.22729 for a level of significance 0.05 supports our conclusion that the "3132 and 3045 cm^{-1}" cluster's spectra density increase has to be attributed to "chemical phenomena" and not to the stochasticity of experimental results (Table 5). A similar ANOVA test performed for normalized power densities for the second sample (PLA) shows a noticeable difference between the means and their variations for two clusters with a coefficient of variation of 0.45. The F factor of 4.21955 for a level of significance 0.05 indicates that the variances in the reflection power densities in two different spectral line clusters also have a statistically significant difference with a probability of 97.767% (Table 4). The increase in the spectral density in the studied range of 3145–3045 cm^{-1} similarly appears to be strongly attributed to the "chemical phenomena" of newly appeared spectra density peaks.

Table 4. One-way ANOVA for PLA samples under UV radiation at 0, 2, 5, 24, and 144 h.

Descriptive Statistics					
	N Analysis	**N Missing**	**Mean**	**Standard Deviation**	**SE of Mean**
PLA 3045	5	0	0.49364	0.43882	0.19625
PLA 3145	5	0	0.39137	0.44599	0.19945
PLA 1379	5	0	0.91441	0.064	0.02862
PLA 1458	5	0	0.9606	0.03875	0.01733
One Way ANOVA					
Overall ANOVA					
	DF	Sum of Squares	Mean Square	F Value	Prob>F
Model	3	1.2566	0.41887	4.21955	0.02233
Error	16	1.58828	0.09927		
Total	19	2.84488			
Null Hypothesis: The means of all levels are equal Alternative Hypothesis: The means of one or more levels are different. At the 0.05 level, the population means are significantly different. Fit Statistics					
R-Square		Coeff Var		Root MSE	Data Mean
0.4417		0.45662		0.31507	0.69

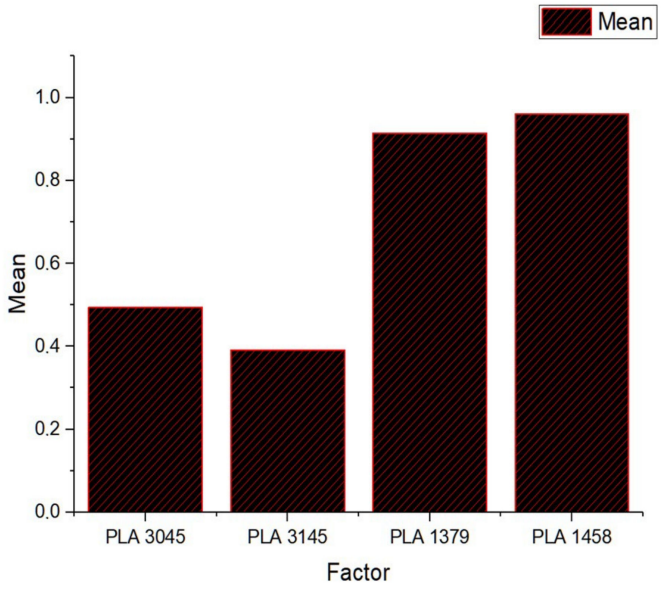


Figure 8. Bar chart.

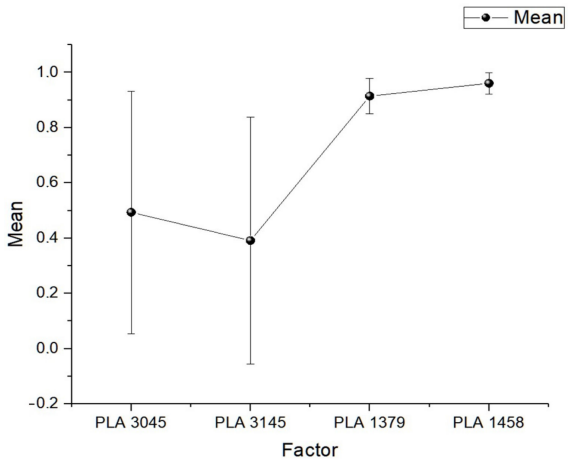


Figure 9. Means Plot SD (as error).

Table 5. One-way ANOVA for PHB samples under UV radiation at 0, 2, 5, 24, and 144 h.

Descriptive Statistics					
	N Analysis	**N Missing**	**Mean**	**Standard Deviation**	**SE of Mean**
PLA 3045	5	0	0.2085	0.44265	0.19796
PLA 3145	5	0	0.20927	0.44212	0.19772
PLA 1379	5	0	0.98746	0.00955	0.00427
PLA 1458	5	0	0.98145	0.02464	0.01102
One Way ANOVA					
Overall ANOVA					
	DF	Sum of Squares	Mean Square	F Value	Prob>F
Model	3	3.00764	1.00255	10.22729	5.3002×10^{-4}
Error	16	1.56843	0.09803		
Total	19	4.57697			
Null Hypothesis: The means of all levels are equal Alternative Hypothesis: The means of one or more levels are different. At the 0.05 level, the population means are significantly different. Fit Statistics					
R-Square		Coeff Var		Root MSE	Data Mean
0.65725		0.52473		0.31309	0.59667

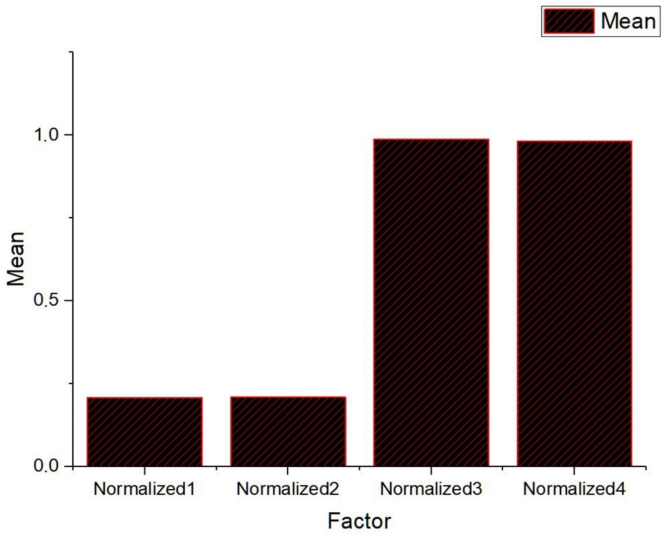


Figure 10. Bar Chart.

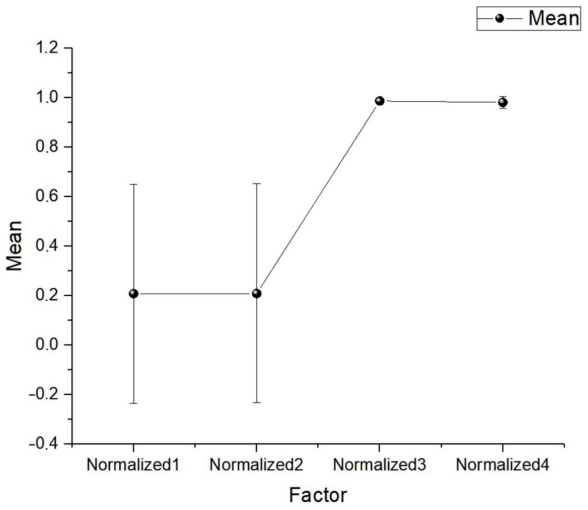


Figure 11. Means Plot SD (as error).

4. Conclusions

The replacement of synthetic polymer materials produced from raw petroleum, which negatively influences the environment, by the ecofriendly polymer composite materials produced from the biodegradable polymers of different classes is an important modern task. The biodegradable binary compositions of the polyesters polylactide (PLA) and poly(3-hydroxybutyrate) (PHB) were synthesized from natural raw materials by chemical and microbiological methods, respectively, with polysaccharide chitosan being successfully used as an effective industrial sorbent of the heavy metal ions from aqueous media as well as for food packaging. The development of composites based on these polyesters and chitosan allows one to join the mechanical characteristics of these polyesters, which are close to characteristics of synthetic polymers, with the high sorption capacity of chitosan. Additionally, the important advantage of such compositions is their capacity to degrade into harmless substances after the end of their service life.

1. The evaluation of the sorption efficiency of both compositions as sorbents by the method of X-ray fluorescence analysis allowed to establish that the sorption of Fe^{3+} ions by PHB–chitosan compositions from aqueous solutions is almost twice as high as that by PLA–chitosan (2.30 and 0.66 wt. %, correspondingly after sorption from 0.008 mol/L $FeCl_3$ solution during 24 h). This effect is connected with a lower crystallinity of PLA compared with PHB (43.2% and 63.5%, correspondingly), which was established under the study of the thermophysical characteristics of both compositions by DSC method and as a sequence with their various influence on the sorption activity of chitosan.
2. The DSC analysis of the PLA–chitosan composition and this composition containing sorbed iron ions showed a slight decrease in the values of T_g (62.8 °C and 61.3 °C, respectively), T_{cc} (113.7 °C and 107 °C, respectively), and T_m (Table 2) as well as an increase in the enthalpy of cold crystallization and a reduction in the degree of crystallinity χ (24.6 and 22.9%, respectively). The DSC analysis of the PHB–chitosan and PHB–chitosan composition containing sorbed iron ions showed a minor decrease in T_m (Table 2) as well as a reduction in the degree of crystallinity χ (51.5 and 50.0%, respectively).
3. High-temperature DSC studies of PHB–chitosan and PLA–chitosan compositions showed the destabilizing effect of chitosan on their thermal stability (Table 3). The reason for such a significant decrease in the thermal stability of PLA and PHB in their compositions with chitosan is connected with the presence of free amino groups in the molecule of chitosan, which accelerates the hydrolysis and depolymerization of linear polyesters.
4. The structural changes in PLA and PHB polyesters subjected to UV radiation were studied with the use of FTIR and significant changes in the spectrum were observed. Based on the analysis of the IR spectra of PHB and PLA, it was concluded that, under the action of UV radiation, the scission of ester bonds takes place, as expressed in the appearance of intense bands characterizing the formation of new structural units, leading to the decrease in the molecular weight of polyesters. It is shown that the photodegradation process of PHB mainly occurs in the amorphous phase of the polymer.
5. The one-way ANOVA statistical analysis of FTIR data, related to the most significant results, confirmed the validity of the conclusion on the formation of bands appearing in the spectra (–OH stretching vibrations of the carboxyl group) as a sequence of the predominant breaking of ester bonds during the photodegradation of PLA and PHB.

Thus, the presented results demonstrate how this application obtained materials which are ecofriendly industrial sorbents which could be used in food packaging materials, but also necessitates further investigations for the creation of completely biodegradable polymer articles.

The study of investigated systems should be continued, and in the future, these authors propose to study the influence of UV radiation on the structure of PLA and PHB

by SEM and NMR methods, while the change in molecular weight would be measured by the method of gel permeation chromatography (GPC), which makes it possible to obtain more complete data about the changes occurring in polyesters under UV action.

Supplementary Materials: The following supporting information can be downloaded at: https://www.mdpi.com/article/10.3390/app13063920/s1, Figure S1: The range 1500–1200 cm^{-1} of the IR spectrum of PHB after UV irradiation (hours): 0 (A), 2 (B), 5 (C), 24, (D), 144 (E); Table S2: Spectral assignment in the range of 1500–1200 cm^{-1} of the PHB IR spectrum; Figure S3: IR spectrum of PHB after UV irradiation. The range of the vibrational spectrum related to the C=O carbonyl group (1724 cm^{-1} [37] - the original PHB; bands in the range of 1743 cm^{-1} appear as a result of UV irradiation (hours): 0 (A), 2 (B), 5 (C), 24, (D), 144 (E)); Figure S4: The range 1200–1000 cm^{-1} of the IR spectrum of PHB after UV irradiation (hours): 0 (A), 2 (B), 5 (C), 24, (D), 144 (E); Table S5: Spectral assignment in the range of 1200–1000 cm^{-1} of the PHB IR spectrum; Figure S6: The range 1000–800 cm^{-1} of the IR spectrum of PHB after UV irradiation (hours): 0 (A), 2 (B), 5 (C), 24, (D), 144 (E); Table S7: Spectral assignment in the range of 1000–800 cm^{-1} of the PHB IR spectrum; Figure S8: The range 1250–1000 cm^{-1} of the IR spectrum of PLA after UV irradiation (hours): 0 (A), 2 (B), 5 (C), 24, (D), 144 (E); Table S9: Spectral assignment in the range of 1250–1000 cm^{-1} of the PLA IR spectrum; Figure S10: The range 1500–1200 cm^{-1} of the IR spec-trum of PLA after UV irradiation (hours): 0 (A), 2 (B), 5 (C), 24, (D), 144 (E); Table S11: Spectral assignment in the range of 1500–1200 cm^{-1} of the PLA IR spectrum; Figure S12: IR spectrum of PLA after UV irradiation. The range of the vibrational spectrum related to the C=O carbonyl group (1753 cm^{-1} [37,38]- the original PLA; bands in the range of 1724 cm−1 appear as a result of UV irradiation (hours): 0 (A), 2 (B), 5 (C), 24, (D), 144 (E)).

Author Contributions: Conceptualization, S.R.; Data curation, S.R.; Funding acquisition, S.L.; Investigation, L.Z., A.Y., S.L. and S.U., Methodology, L.Z. and S.L.; Project administration, A.B.; Supervision, A.B.; Validation, L.Z.; Visualization, L.Z.; Writing—original draft, L.Z.; Writing—review and editing, S.R. All authors have read and agreed to the published version of the manuscript.

Funding: This work was performed under financial support from the Ministry of Education and Science of the Russian Federation (contract no. FFZE-2022-0010).

Institutional Review Board Statement: Not applicable.

Informed Consent Statement: Informed consent was obtained from all subjects involved in the study.

Data Availability Statement: The data presented in this study are available upon request from the corresponding author.

Conflicts of Interest: The authors declare no conflict of interest.

References

1. Flury, M.; Narayan, R. Biodegradable plastic as an integral part of the solution to plastic waste pollution of the environment. *Curr. Opin. Green Sustain. Chem.* **2021**, *30*, 100490. [CrossRef]
2. Moshood, T.D.; Nawanir, G.; Mahmud, F.; Mohamad, F.; Ahmad, M.H.; Ghani, A.A. Biodegradable plastic applications towards sustainability: A recent innovations in the green product. *Clean. Eng. Technol.* **2022**, *6*, 100404. [CrossRef]
3. Kumar, S.R.; Shaiju, P.; O'Connor, K.E.; Babu, R. Bio-based and biodegradable polymers—State-of-the-art, challenges and emerging trends. *Curr. Opin. Green Sustain. Chem.* **2020**, *21*, 75–81. [CrossRef]
4. Haldar, D.; Duarah, P.; Purkait, M.K. MOFs for the treatment of arsenic, fluoride and iron contaminated drinking water: A review. *Chemosphere* **2020**, *251*, 126388. [CrossRef]
5. Zhang, L.; Zeng, Y.; Cheng, Z. Removal of heavy metal ions using chitosan and modified chitosan: A review. *J. Mol. Liq.* **2016**, *214*, 175–191. [CrossRef]
6. Zhang, Y.; Zhao, M.; Cheng, Q.; Wang, C.; Li, H.; Han, X.; Fan, Z.; Su, G.; Pan, D.; Li, Z. Research progress of adsorption and removal of heavy metals by chitosan and its derivatives: A review. *Chemosphere* **2021**, *279*, 130927. [CrossRef]
7. Aranaz, I.; Alcantara, A.; Civera, M.; Arias, C.; Elorza, B.; Caballero, A.; Acosta, N. Chitosan: An Overview of Its Properties and Applications. *Polymers* **2021**, *13*, 3256. [CrossRef]
8. Velasquez, C.; Albornoz, J.; Nava, J.; Barrios, E.; Velasquez, H. Conductimetric studies of chitosan in aqueous medium. *Polym. Bull.* **2005**, *55*, 201–208. [CrossRef]
9. Auras, R.; Harte, B.; Selke, S. A review of polylactides as packing materials. *Macromol. Biosci.* **2004**, *4*, 835–864. [CrossRef]
10. Widiastuti, I. Polylactides nanocomposites for packing materials: A review. *AIP Conf. Proc.* **2016**, *1710*, 030020. [CrossRef]

11. Ahmed, J.; Varshney Sunil, K. Polylactides—Chemistry, Properties and Green Packaging Technology: A review. *Int. J. Food Prop.* **2011**, *14*, 37–58. [CrossRef]
12. Spierling, S.; Knupfer, E.; Behsen, H.; Mudersbach, M.; Krieg, H.; Springer, S. Bio-based plastics—A review of environmental, social and economic impact assessments. *J. Clean. Prod.* **2018**, *185*, 476–491. [CrossRef]
13. Tian, K.; Bilal, M. Research progress of biodegradable materials in reducing environmental pollution. *Abat. Environ. Pollut.* **2020**, *30*, 313–330. [CrossRef]
14. Zhong, Y.; Godwin, P.; Jinm, Y.; Xiao, H. Biodegradable polymers and green-based antimicrobial hacking materials: A mini-review. *Adv. Ind. Eng. Polym. Res.* **2019**, *3*, 27–35. [CrossRef]
15. European Bioplastics. Bioplastic Market Development Update 2021. Press Release 2021. Available online: https://www.european-bioplastics.org/global-bioplastics-prosuction-will-more-than-triple-within-thq-next-five-years/ (accessed on 26 September 2022).
16. Alves, M.I.; Macagnan, K.; Rodrigues, A.A.; De Assis, D.A.; Torres, M.M.; De Oliveira, P.D.; Furlan, L.; Vendruscolo, C.T.; Moreira, A.D.S. Poly(3-hydroxybutyrate)-P(3HB): Review of Production Process Technology. *Ind. Biotechnol.* **2017**, *13*, 192–208. [CrossRef]
17. Chen, Y.; Geever, L.; Killion, J.; Lyons, J. A review of multifarious Applications of Poly (Lactic Acid). *Polym. Plast. Technol. Eng.* **2016**, *55*, 1057–1075. [CrossRef]
18. Shetty, S.; Shetty, N. Investigation of medical properties and applications of polylactic acids—A review. *Mater. Res. Express* **2019**, *6*, 1120202. [CrossRef]
19. Folino, A.; Karageorgio, A.; Calabro, P.S.; Komilis, D. Biodegradationof wasted bioplastics in natural and industrial enviroments: A review. *Sustainability* **2020**, *12*, 6030. [CrossRef]
20. Rhein, S.; Schmid, M. Consumers' awareness of plastic packing: More than just environmental concerns. *Resour. Conserv. Recycl.* **2020**, *162*, 105063. [CrossRef]
21. Chirilli, C.; Molino, M.; Torri, L. Consumers' awareness, behavior and expectations for food packaging environmental sustainability: Influence of socio-demographic characteristics. *Foods* **2022**, *11*, 2388. [CrossRef]
22. Zhorina, L.; Rogovina, S.; Prut, E.; Kuznetsova, O.; Grachev, A.; Ivanushkina, N.; Iordansky, A.; Berlin, A. Biodegradable compositions based on poly-(3-hydroxybutyrate) and polylactide polyesters produced vegetable raw materials. *Polym. Sci. Ser. A* **2020**, *62*, 361–367. [CrossRef]
23. Rogovina, S.; Zhorina, L.; Iordansky, A.; Prut, E.; Yakhina, A.; Grachev, A.; Berlin, A.; Shapagin, A. New biodegradable absorbents based on polylactide, poly(3-hydroxybutyrate), and chitosan for sorption of iron and chromium ions. *Polym. Sci. Ser. A* **2021**, *63*, 804–814. [CrossRef]
24. Rogovina, S.; Zhorina, L.; Iordansky, A.; Yakhina, A.; Shapagin, A.; Berlin, A. Hydrolysis, Biodegradation and Ion Sorption in Binary Biocomposites of Chitosan with Polyesters: Polylactide and Poly(3-Hydroxybutyrate). *Polymers* **2023**, *15*, 645. [CrossRef] [PubMed]
25. Csapo, J.; Prokisch, J.; Albert, C.; Sipos, P. Effect of UV light on food quality and safety. *Acta Univ. Sapientiae Aliment.* **2019**, *12*, 21–41. [CrossRef]
26. Darre, M.; Vicente, A.; Cisneros-Zevallos, L.; Artes-Hernandez, F. Postharvest ultraviolet radiation in fruit and vegetables: Applications and factors modulating its efficacy on bioactive compounds and microbial grown. *Foods* **2022**, *11*, 653. [CrossRef]
27. Fischer, E.; Sterzel, H.; Wegner, G. Investigation of the structure of solution grown crystals of lactide copolymers by means of chemical reactions. *Colloid Polym. Sci.* **1973**, *521*, 980–990. [CrossRef]
28. Barham, P.J.; Keller, A.; Otun, E.L.; Holmes, P.A. Crystallization and morphology of a bacterial thermoplastic: Poly-3-hydroxybutyrate. *J. Mater. Sci.* **1984**, *19*, 2781–2794. [CrossRef]
29. Pereira, F.; Lanfredi, S.; Gonzalez, E.; Agostini, D.; Gomes, H.; Medeiros, R.S. Thermal and morphological study of chitosan metal complexes. *J. Therm. Anal. Calorim.* **2017**, *129*, 291–301. [CrossRef]
30. Pereira, F.; Agostini, D.; Job, A.; Gonzalez, E. Thermal studies of chitin–chitosan derivatives. *J. Therm. Anal. Calorim.* **2013**, *114*, 321–327. [CrossRef]
31. Furukawa, T.; Sato, H.; Murakami, R.; Zhang, J.; Duan, Y.; Noda, I.; Ochiai, S.; Ozaki, Y. Structure, Dispersibility, and Crystallinity of Poly(hydroxybutyrate)/Poly(L-lactic acid) Blends Studied by FT-IR Microspectroscopy and Differential Scanning Calorimetry. *Macromolecules* **2005**, *38*, 6445–6454. [CrossRef]
32. Kann, Y.; Shurgalin, M.; Krishnaswamy, R. FTIR spectroscopy for analysis of crystallinity of poly(3-hydroxybutyrate-c o-4 -hydroxybutyrate) polymers and its utilization in evaluation of aging, orientation and composition. *Polym. Testing.* **2014**, *40*, 218–224. [CrossRef]
33. Hadži, D.; Sheppard, N. The infra-red absorption bands associated with the COOH and COOD groups in dimeric carboxylic acids. I. The region from 1500 to 500 cm^{-1}. *Proc. R. Soc. London. Ser. A Math. Phys. Sci.* **1953**, *216*, 247–266. [CrossRef]
34. Bratož, S.; Hadži, D.; Sheppard, N. The infra-red absorption bands associated with the COOH and COOD groups in dimeric carboxylic acid -II. The region from 3700 to 1500 cm^{-1}. *Spectrochim. Acta* **1956**, *8*, 249–261. [CrossRef]
35. Padermshoke, A.; Katsumoto, Y.; Sato, H.; Ekgasit, S.; Noda, I.; Ozaki, Y. Melting behavior of poly(3-hydroxybutyrate) investigated by two-dimensional infrared correlation spectroscopy. *Spectrochim. Acta Part A Mol. Biomol. Spectrosc.* **2005**, *61*, 541–550. [CrossRef]
36. Zhang, J.; Sato, H.; Noda, I.; Ozaki, Y. Conformation Rearrangement and Molecular Dynamics of Poly(3-hydroxybutyrate) during the Melt-Crystallization Process Investigated by Infrared and Two-Dimensional Infrared Correlation Spectroscopy. *Macromolecules* **2005**, *38*, 4274–4281. [CrossRef]

37. Kister, G.; Cassanas, G.; Vert, M. Effects of morphology, conformation and configuration on the IR and Raman spectra of various poly(lactic acid)s. *Polymer* **1998**, *39*, 267–273. [CrossRef]
38. Yuniarto, K.; Purwanto, Y.A.; Purwanto, S.; Welt, B.A.; Purwadaria, H.K.; Sunarti, T.C. Infrared and Raman studies on polylactide acid and polyethylene glycol-400 blend. In *AIP Conference Proceedings*; AIP Publishing LLC: Melville, NY, USA, 2016; Volume 1725, p. 020101. [CrossRef]
39. Meaurio, E.; López-Rodríguez, N.; Sarasua, J. Infrared Spectrum of Poly(L-lactide): Application to Crystallinity Studies. *Macromolecules* **2006**, *39*, 9291–9301. [CrossRef]

Disclaimer/Publisher's Note: The statements, opinions and data contained in all publications are solely those of the individual author(s) and contributor(s) and not of MDPI and/or the editor(s). MDPI and/or the editor(s) disclaim responsibility for any injury to people or property resulting from any ideas, methods, instructions or products referred to in the content.